



International Congress of Science and Technology of Metallurgy and Materials, SAM -  
CONAMET 2013

## Talc Nanoparticles Influence on Thermoplastic Corn Starch Film Properties

Olivia López<sup>a,b\*</sup>, Luciana Castillo<sup>a</sup>, Noemí Zarithzky<sup>b</sup>, Silvia Barbosa<sup>a</sup>, Marcelo Villar<sup>a</sup>,  
María Alejandra García<sup>b</sup>

<sup>a</sup>Planta Piloto de Ingeniería Química, PLAPIQUI (UNS-CONICET), Departamento de Ingeniería Química, UNS, Camino La Carrindanga km. 7, (8000) Bahía Blanca, Argentina.

<sup>b</sup>Centro de Investigación y Desarrollo en Criotecnología de Alimentos, CIDCA (UNLP-CONICET), Facultad de Ciencias Exactas, UNLP, 47 y 116, (1900) La Plata, Argentina.

### Abstract

Composite films of TPS with talc nanoparticles were obtained by thermo-compression in order to study the effect of this filler on structure, optical, and thermal properties. TPS-talc films showed good appearance and homogeneous thickness. Talc addition increased the amount of rigid phase in nanocomposite films, thus their cross-sections resulted more irregular than those of TPS ones. Talc preferential orientation within matrix and good compatibility between particles and TPS were evidenced. TEM observation showed scattered randomly dispersed individual talc platelets. Matrix crystallinity degree was not significantly affected by particles presence. Nanocomposite films were optically transparent due to the laminar morphology and nanosized particles. Materials microstructure presented glycerol- and starch-rich domains. Talc incorporation higher than 3 % w/w increased softening resistance of nanocomposites as stated by DMA assays. TPS relaxation temperature of glycerol-rich phase was shifted to higher values since talc nanoparticles reduce starch chains mobility.

© 2015 The Authors. Published by Elsevier Ltd. This is an open access article under the CC BY-NC-ND license (<http://creativecommons.org/licenses/by-nc-nd/4.0/>).

Selection and peer-review under responsibility of the scientific committee of SAM - CONAMET 2013

**Keywords:** Thermoplastic corn starch; Talc nanoparticles; Films; Microstructural characterization; Optical properties

\* Corresponding author. Tel.: +54-291-486-1700; fax: +54-291-486-1600.  
E-mail address: [olivialopez@plapiqui.edu.ar](mailto:olivialopez@plapiqui.edu.ar)

## 1. Introduction

Actually, biomaterials development for food packaging is focused on the reduction of environmental impact either in their processing and final disposal. Main advantages of these materials are their precedence from renewable sources and their biodegradable character. In this context, the use of starches of different botanical origins for films and coatings developments was reported by several authors, demonstrating the potential of this polysaccharide (López and García, 2012; Müller et al., 2009). Native starch presents a granular structure, which can be disrupted and converted into thermoplastic starch (TPS) by processing under high temperature and shear conditions in presence of plasticizers (Da Silva Pinto et al., 2009). Taking into account starch hydrophilic nature, TPS based materials show certain drawbacks related to their mechanical performance and water vapor permeability (Averous and Boquillon, 2004). In order to overcome these limitations, different natural and mineral filler addition to TPS matrixes enhances their mechanical and barrier properties (Müller et al., 2009; Wilhelm et al., 2003). Besides, fillers presence also modifies TPS films optical properties, as well as, their structure and morphology, determining their final applications. In this sense, several clays were used to reinforce starch matrixes (Tunjano et al., 2009; Wilhelm et al., 2003). Talc mineral could be used as TPS filler considering that it qualifies as good reinforcement agent of polymeric matrixes due to its layered morphology and nanometric thickness with high aspect ratio (Castillo et al., 2012).

The aim of the present work was to evaluate the effect of talc nanoparticles addition on microstructure of thermoplastic corn starch. Besides, talc influence on films optical and thermal properties was also investigated.

## 2. Materials and Methods

### 2.1. Materials

Native corn starch was provided by Misky-Arcor (Tucumán, Argentine) with an amylose content of  $23.9 \pm 0.7$  % (López et al., 2008). Talc sample was supplied by Dolomita SAIC (Argentine). This mineral comes from an Australian ore, having a high purity (98 %), median diameter  $d_{50}$  of  $5.9 \pm 3.8$   $\mu\text{m}$  (particle diameter at which 50 % of the sample is finer than) and nanometric thickness of  $79 \pm 16$  nm. Glycerol (Anedra, Argentine) was used as plasticizer.

### 2.2 Thermoplastic starch mixtures

Mixtures of native corn starch, glycerol (30 % w/w), distilled water (45 % w/w) and talc nanoparticles (0, 1.7, 5.2 and 8.7 % w/w) were prepared. Composition was expressed in g per 100 g of starch, which implies that 0, 1, 3 and 5 % w/w talc respect to TPS were used. Talc was premixed with starch to achieve good particle dispersion between both powders. Then, glycerol and distilled water were added and samples were mixed and conditioned at 25 °C during 24 h. After that, conditioned mixtures were processed in a Brabender Plastograph (Brabender, Germany) at 140 °C and 50 rpm for 15 min. Processed mixtures were removed from the mixing chamber, triturated and conditioned at 25 °C and 60 % relative humidity (RH), in order to improve their future procesability.

### 2.3 Films preparation

Thermoplastic starch films were obtained by thermo-compression using a hydraulic press. Processing conditions were  $150 \text{ kg}\cdot\text{cm}^{-2}$  at 140 °C during 6 min. An aluminum support as frame of 1 mm thickness and a molding relation of 3 g sample per  $\text{cm}^3$  was used. Material was cooled under pressure up to approximately 50 °C; then the pressure was released and obtained films were removed from the frames. Before characterization, films were conditioned at 25 °C and 60 % RH. Films thickness was measured at different locations of the specimens, employing a micrometer and ten measurements were taken on each film, reporting the mean values.

## 2.4 Structural aspects

Talc nanoparticles distribution in TPS matrix, as well as, homogeneity and appearance of developed films were studied by Scanning Electron Microscopy (SEM). This characterization was performed in a JEOL JSM-35 CF electron microscope (Japan), with a secondary electron detector. Films were cryofractured by immersion in liquid nitrogen, mounted on bronze stubs and coated with a gold layer (~30 Å), using an argon plasma metallizer (sputter coater PELCO 91000).

Transmission electron microscopy (TEM) was performed in order to analyze the dispersion of talc layers. Samples were microtomed at room temperature using an ultramicrotome LKB Ultratome 2088 (KB-Produkter AB., Bromma, Sweden) equipped with a diamond knife. Ultrathin sections (~1000 Å) were picked up using a copper grid. Samples were examined using a JEOL 100 CX (JEOL USA, Inc.) operating at an acceleration voltage of 100 kV.

## 2.5 Optical properties

Opacity and UV barrier capacity of films were spectrophotometrically determined. Absorbance spectrum (200–700 nm) was recorded using a SHIMADZU UV-160 (Japan) spectrophotometer. Films were cut into rectangles (3 x 1 cm) and placed on the internal side of a quartz spectrophotometer cell. Film opacity (AU nm) was defined as the area under the recorded curve determined by an integration procedure according to standard test method ASTM D1003-00. Filler blocking effect to UV and visible transmission was calculated with the equation proposed by Sanchez-Garcia et al. (2010) as follows:

$$\text{Blocking effect} = \frac{(T_{TPS} - T_{NANOCOMPOSITE})}{m_t} \quad (1)$$

where  $T_{TPS}$  and  $T_{NANOCOMPOSITE}$  refer to percent transmittance for TPS and nanocomposite films, respectively and  $m_t$  is talc percent respect to starch mass. Blocking effect was calculated for three wavelengths 300, 350 and 750 nm in UV-B, UV-A and visible region, respectively (Mbey et al., 2012).

Films color measurements were performed using a Hunterlab UltraScan XE (USA) colorimeter in the transmittance mode. Color parameters  $L$ ,  $a$  and  $b$  were recorded according to the Hunter scale, in at least ten randomly selected positions for each specimen. Color parameters range from  $L = 0$  (black) to  $L = 100$  (white),  $-a$  (greenness) to  $+a$  (redness) and  $-b$  (blueness) to  $+b$  (yellowness). Standard values considered were those of the white background ( $L = 97.75$ ,  $a = -0.49$ , and  $b = 1.96$ ). Besides,  $\Delta L$ ,  $\Delta a$ , and  $\Delta b$  were calculated, taking into account the standard values of the white background and the parameter color difference ( $\Delta E$ ) was also determined as follows:

$$\Delta E = \sqrt{\Delta L^2 + \Delta a^2 + \Delta b^2} \quad (2)$$

## 2.6 Dynamic mechanical behavior

Temperatures and intensities of relaxation phenomena of films were determined by Dynamic Mechanical Analysis (DMA). Assays were carried out in a dynamic-mechanical thermal equipment Q800 (TA Instruments, New Castle, USA) with a liquid nitrogen cooling system, using a clamp tension. Multi-frequency sweeps at fixed amplitude from -100 to 100 °C at 2 °C/min were carried out. Storage ( $E'$ ) and loss ( $E''$ ) moduli as well as  $\tan \delta$  curves as a function of temperature were recorded and analyzed using the software Universal Analysis 2000.  $E'$  is related to the mechanical energy stored per cycle when the sample is subjected to a deformation and it is the elastic response of the material.  $E''$  is the viscous response which is related to the energy dissipated as heat per cycle when

the sample is deformed. Loss factor is defined as  $\tan \delta = E''/E'$ , being  $\delta$  the angle between the in-phase and out-of-phase components of the modulus in the cyclic motion. Temperatures of the relaxation processes associated to glass transition temperatures ( $T_g$ ) were determined through the inflexion point of the storage modulus  $E'$  curve as well as the maximum peak in both the loss modulus  $E''$  and  $\tan \delta$  curves (Psomiadou et al., 1996).

### 2.7 Statistical analysis

A completely randomized experimental design was used to characterize nanocomposite films. Analysis of variance (ANOVA) was used to compare mean differences of samples properties. Besides, comparison of mean values was performed by Fisher's least significant difference test conducted at a significance level  $p = 0.05$ .

## 3. Results and discussion

Films based on TPS-talc nanoparticles were homogeneous and easy to handle, with good appearance and constant thickness (196 -214  $\mu\text{m}$ ). Thermo-compression process allowed obtaining films with controlled thickness, being this parameter significant in materials structure study and its relation to their final properties.

### 3.1 Talc nanoparticles effect on TPS films microstructure

Fig. 1 shows SEM micrographs corresponding to films cryofractured surface. Homogeneous appearance was observed for TPS films without talc. Starch granules lack indicates thermo-compression process effectiveness (Fig. 1a). On the other hand, films based on TPS with talc also presented homogenous cross-sections evidencing a good particle distribution (Figs. 1b, 1c and 1d). This feature favors a higher matrix-filler superficial area modifying polymeric chains mobility and relaxation behavior as well as mechanical and thermal properties (De Azeredo, 2009). Despite particles were not surface modified, high TPS-talc compatibility was evidenced by the good interfacial adhesion between matrix and this inorganic filler. Moreover, preferential orientation of talc particles was detected as a consequence of filler lamellar morphology and thermo-compression process. Talc incorporation modified fracture surfaces of TPS films, increasing cross-section irregularity with filler concentration (Figs. 1b, 1c and 1d). This result was expected due to talc addition raises rigid phase amount of these materials. Glycerol loss was negligible since processing temperature was lower than plasticizer boiling point. Besides, SEM micrographs not showed typical channels of glycerol migration (López et al., 2011).

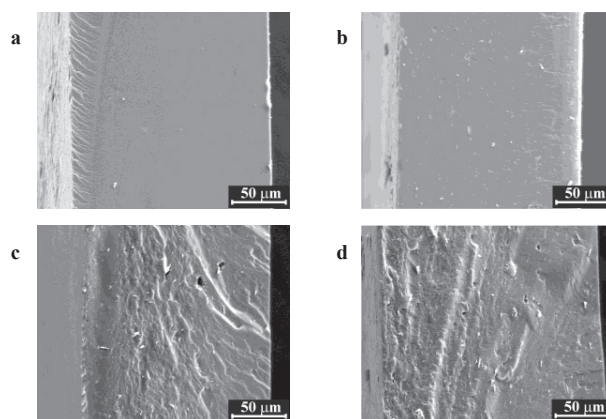


Fig 1. SEM micrographs (540x) of TPS films with (a) 0, (b) 1, (c) 3 and (d) 5 % w/w talc nanoparticles.

Nanocomposites internal structure and talc particles spatial dispersion within TPS matrix were evaluated by TEM. Fig. 2 shows representative TEM micrographs at two different magnifications corresponding to nanocomposites with 3 % w/w talc. Individual and intercalated talc platelets dispersed along TPS matrix were

observed. Moreover, nanocomposites TEM micrographs revealed nanometric thickness of the individual laminar particles. Fig. 2a corresponds to a micrograph at low magnification showing heterogeneous morphology that contains talc nanoparticles rich domains and other regions without filler presence. Chivrac et al. (2009) reported similar results for starch nanocomposites with montmorillonite. In this sense, Avérous (2004) emphasized that this result could be associated to the high glycerol content which induces phase separation between domains having high and low plasticizer content. Individual particles presence could indicate some interaction degree between talc silanol (Si-OH) and starch hydroxyl groups by hydrogen bonding, favoring nanofiller dispersion (Chivrac et al., 2009). In Fig. 2b, an incipient TPS intercalation among talc nanoparticles is observed.

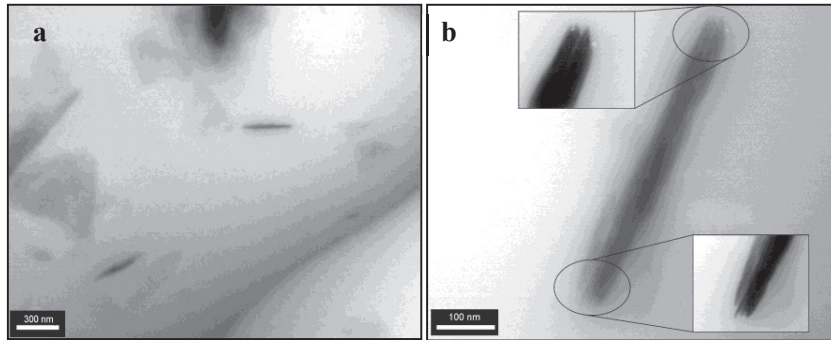


Fig. 2. TEM micrographs of films based on thermoplastic corn starch with 3 % w/w talc nanoparticles at: (a) 20000x and (b) 200000x.

### 3.2 Optical properties of TPS-talc films

Taking into account that these films could be used to develop packages, optical properties condition their final applications. As it shown in Fig. 3 it could be appreciate that nanocomposite films resulted translucent with low color development increasing film opacity with talc content.

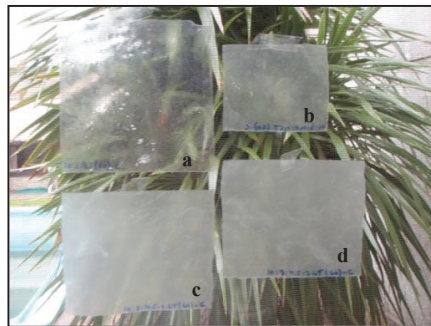


Fig. 3. Photographs of TPS films with: (a) 0, (b) 1, (c) 3 and (d) 5 % w/w talc particles.

TPS films color parameters are presented in Table 1. Talc nanoparticles modified luminosity ( $L$ ) as well as chromaticity values ( $a$  and  $b$ ) of TPS films. Filler addition higher than 3 % w/w reduced significantly ( $p < 0.05$ ) films luminosity, this fact is also observed in Fig.3 as it was previously indicated. Besides, nanocomposite had lower  $a$  values (red-green), while  $b$  parameter (yellow-blue) resulted significantly higher, compared to those corresponding to TPS. Other chromaticity parameter which shows combined effects of  $L$ ,  $a$  and  $b$  is defined as color difference ( $\Delta E$ ) which is also included in Table 1. Adding 3 % w/w talc nanoparticles to TPS matrix altered significantly ( $p < 0.05$ )  $\Delta E$  values.

Table 1. Color parameters and opacity of TPS films with talc nanoparticles.

TPS film's talc content (% w/w)	Color parameters				Opacity (AU x nm)
	<i>L</i>	<i>a</i>	<i>b</i>	$\Delta E$	
0	85.4±0.2 <sup>a</sup>	8.00±0.02 <sup>a</sup>	1.6±0.1 <sup>a</sup>	85.8±0.2 <sup>a</sup>	31.8±6.4 <sup>a</sup>
1	85.0±0.4 <sup>a,b</sup>	7.88±0.06 <sup>b</sup>	2.1±0.3 <sup>b</sup>	85.4±0.5 <sup>a,b</sup>	54.5±6.7 <sup>b</sup>
3	84.5±0.4 <sup>b</sup>	7.88±0.05 <sup>b</sup>	2.4±0.3 <sup>b</sup>	84.9±0.5 <sup>b</sup>	71.6±2.1 <sup>c</sup>
5	83.1±0.5 <sup>c</sup>	7.83±0.05 <sup>b</sup>	4.3±0.4 <sup>c</sup>	83.6±0.6 <sup>c</sup>	109.0±9.3 <sup>d</sup>

Reported values correspond to the mean  $\pm$  standard deviation. Values within each column followed by different letters indicate significant differences ( $p < 0.05$ ).

Evaluation of UV absorption capacity of developed films is relevant in order to propose possible applications of these materials, especially in food packaging area. Fig. 4a corresponds to UV-vis spectra of TPS films with all studied talc concentrations. Spectra presented an absorption peak located between 270 and 300 nm, indicating that talc nanoparticles did not affect UV absorption capacity of TPS films. Materials which are able to absorb in UV zone could be useful to package and extend shelf life of food products which are susceptible to oxidative rancidity catalyzed by UV light. Besides, this study allowed analyzing filler dispersion within matrix giving information about talc blocking effect to UV and visible radiation. Filler blocking effect is presented in Fig. 4b as a function of talc concentration. Filler content higher than 3% w/w reduced significantly ( $p < 0.05$ ) UV and visible light transmission. Similar tendency was reported by Mbey et al. (2012) for cassava starch–kaolinite composite films. Concerning to talc effect on TPS films opacity, it could be appreciate that this property was increased significantly ( $p < 0.05$ ) with talc concentration (Table 1). Despite of mineral presence increased films opacity, their values were low since filler particles are extremely thin, as it could be observed by TEM in Fig.2. Thus, when they are dispersed in TPS matrix, resulting nanocomposites are optically clear.

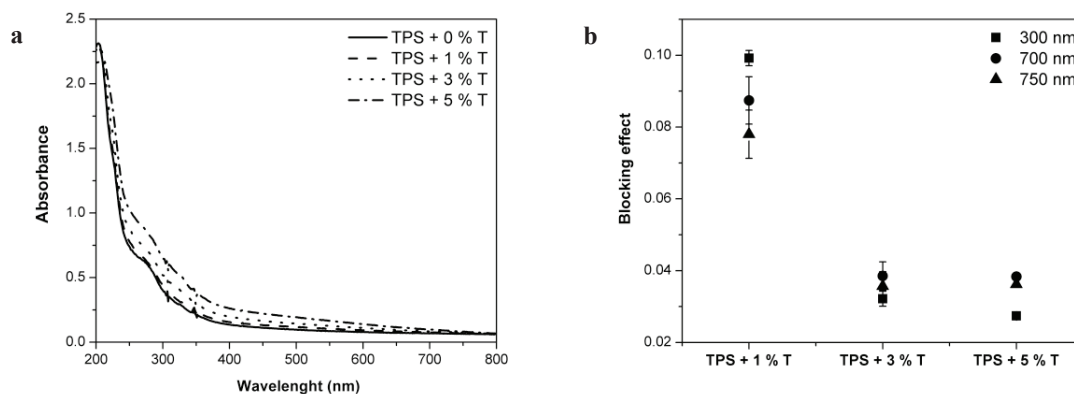


Fig. 4. (a) Absorption spectra (200-700 nm) of TPS films with 0, 1, 3 and 5 % w/w talc nanoparticles (T). (b) Talc blocking effect.

Fig. 5 shows DMA profiles of TPS films and those corresponding to nanocomposite ones. DMA curves of TPS showed two relaxations, one located at lower temperature which is associated to glycerol-rich phase and the second one associated to starch-rich phase. Several authors reported that starch-glycerol mixtures are partially miscible systems, given rise to a starch- and a glycerol-rich phases (López et al., 2011; Mathew & Dufresne, 2002). In the case of TPS films and nanocomposite with 1 % w/w talc, relaxation corresponding to starch-rich phase could not be determined since samples suffered softening during the assays (Fig. 5). It had been reported that the transition corresponding to plasticizer-rich phase for different TPS matrixes has a better definition with a higher intensity change than the second one attributed to the starch-rich phase (López et al., 2011; Wilhelm et al., 2003). An increase of rigid phase amount by addition of 3 and 5 % w/w talc nanoparticles led to a higher softening resistance during measurements, allowing a better definition of the relaxation associated to starch-rich phase in these nanocomposites (Fig. 5).

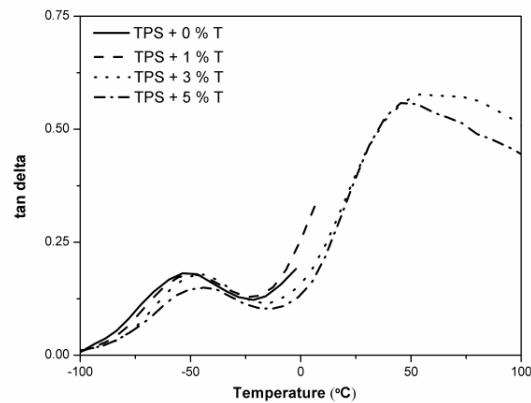


Fig. 5. DMA spectra of thermoplastic corn starch films with talc nanoparticles. Dependence of  $E'$  (storage modulus),  $E''$  (loss modulus) and  $\tan \delta$  with temperature at a constant frequency of 3 Hz.

Besides, the effect of talc addition on TPS dynamic mechanical parameters was also evaluated. Relaxation temperatures associated to glass transitions of glycerol- and starch-rich phases for all developed TPS films are presented in Table 2.

Table 2. Relaxation temperatures of thermoplastic corn starch films (TPS) with talc nanoparticles determined by DMA (3 Hz).

TPS film's talc content (% w/w)	Relaxation temperatures associated to the glass transition of the glycerol-rich phase (°C)		
	Inflexion in storage modulus ( $E'$ )	Maximum in loss modulus ( $E''$ )	Maximum in $\tan \delta$
0	-68.0±0.6 <sup>a</sup>	-60.5±4.1 <sup>a</sup>	-51.8±1.0 <sup>a</sup>
1	-67.3±3.3 <sup>a</sup>	-57.8±5.8 <sup>a</sup>	-51.2±6.0 <sup>a</sup>
3	-53.7±0.8 <sup>b</sup>	-56.9±0.8 <sup>a</sup>	-47.1±5.6 <sup>a</sup>
5	-55.1±3.1 <sup>b</sup>	-58.1±3.0 <sup>a</sup>	-45.4±3.2 <sup>a</sup>
TPS film's talc content (% w/w)	Relaxation temperatures associated to the glass transition of the starch-rich phase (°C)		
	Inflexion in storage modulus ( $E'$ )	Maximum in loss modulus ( $E''$ )	Maximum in $\tan \delta$
0	nd	nd	nd
1	nd	nd	nd
3	9.4±0.7 <sup>a</sup>	30.0±2.6 <sup>a</sup>	46.9±0.8 <sup>a</sup>
5	9.5±0.8 <sup>a</sup>	28.8±4.7 <sup>a</sup>	45.9±0.8 <sup>a</sup>

Reported values correspond to the mean ± standard deviation. Values within each column followed by different letters indicate significant differences ( $p < 0.05$ ). nd: no detected

Despite there is no significant differences ( $p > 0.05$ ) among relaxation temperatures corresponding to glycerol-rich phase, an increase in their mean values with talc concentration were observed. This tendency was found considering storage and loss moduli, as well as,  $\tan \delta$  curves and it could be attributed to chain mobility reduction due to the presence of talc nanoparticles. Similar results were reported by Chivrac et al. (2009) for glass transition temperature of starch rich phase of composites based on starch and clay.  $T_g$  values corresponding to starch-rich phase of TPS and nanocomposite with 1 % w/w talc could not be assessed due to sample softening, as it was previously described. Relaxation temperatures of this phase for TPS films with 3 and 5 % w/w did not show significant ( $p > 0.05$ ) differences between them (Table 2).

#### 4. Conclusions

Films nanocomposite based on thermoplastic corn starch and talc particles were obtained by thermo-compression showing a good appearance and constant thickness as well as smooth and homogenous surfaces. Nanocomposite films presented cross-sections more irregular than TPS ones due to talc nanoparticles addition increased amount of rigid phase. Filler laminar morphology led to a preferential particle orientation within the matrix during thermo-compression process. Individual and intercalated talc platelets distributed along TPS matrix were observed by TEM. Developed materials were optically transparent being able to absorb UV radiation. DMA spectra of TPS films and their nanocomposites exhibited two relaxations related to the partial glycerol-starch miscibility. Starch-rich phase relaxation was more evident for nanocomposites with talc concentrations higher than 3 % w/w since the increased rigid phase allowed a higher softening resistance during assays. Talc nanoparticles restricted starch chains mobility shifting relaxation temperature of glycerol-rich phase to higher values.

The effect of talc addition to TPS matrix was analyzed by several complementary techniques focusing on structural changes and optical properties as well as in dynamic-mechanical behavior. It is expected that these nanocomposites films could be used as materials for biodegradable packaging.

#### References

- Avérous, L. 2004. Biodegradable Multiphase Systems Based on Plasticized Starch: A Review. *Journal of Macromolecular Science, Part C: Polymer Reviews*44(3), 231–274.
- Averous, L., Boquillon, N. 2004. Biocomposites based on plasticized starch: thermal and mechanical behaviours. *Carbohydrate Polymers*56(2), 111–122.
- Castillo, L. A., Barbosa, S. E., Capiati, N. J. 2012. Influence of Talc Genesis and Particle Surface on the Crystallization Kinetics of Polypropylene / Talc Composites. *Journal of Applied Polymer Science* 126, 1763–1772.
- Chivrac, F., Pollet, E., Avérous, L. 2009. Progress in nano-biocomposites based on polysaccharides and nanoclays. *Materials Science and Engineering: R: Reports*67(1), 1–17.
- Da Silva Pinto, C. E., Arizaga, G. G. C., Wypych, F., Ramos, L. P., Satyanarayana, K. G. 2009. Studies of the effect of molding pressure and incorporation of sugarcane bagasse fibers on the structure and properties of poly (hydroxy butyrate). *Composites Part A: Applied Science and Manufacturing*40(5), 573–582.
- De Azeredo, H. M. C. 2009. Nanocomposites for food packaging applications. *Food Research International*42(9), 1240–1253.
- López, O. V., García, M. A. 2012. Starch films from a novel (*Pachyrhizus ahipa*) and conventional sources: Development and characterization. *Materials Science and Engineering: C*32(7), 1931–1940.
- López, O. V., García, M. A., Zaritzky, N. E. 2008. Film forming capacity of chemically modified corn starches. *Carbohydrate Polymers*73(4), 573–581.
- López, O. V., Lecot, C. J., Zaritzky, N. E., García, M. A. 2011. Biodegradable packages development from starch based heat sealable films. *Journal of Food Engineering*105(2), 254–263.
- Mathew, A. P., Dufresne, A. 2002. Morphological investigation of nanocomposites from sorbitol plasticized starch and tunicin whiskers. *Biomacromolecules*3, 609–617.
- Mbey, J. A., Hoppe, S., Thomas, F. 2012. Cassava starch–kaolinite composite film. Effect of clay content and clay modification on film properties. *Carbohydrate Polymers*88, 213–222.
- Müller, C. M. O., Laurindo, J. B., Yamashita, F. 2009. Effect of cellulose fibers addition on the mechanical properties and water vapor barrier of starch-based films. *Food Hydrocolloids*23(5), 1328–1333.
- Psomiadou, E., Arvanitoyannis, I., Yamamoto, N. 1996. Edible films made from natural resources ; microcrystalline cellulose ( MCC ), methylcellulose ( MC ) and corn starch and polyols-Part 2. *Carbohydrate Polymers*31, 193–204.
- Sanchez-Garcia, M. D., Hilliou, L., Lagaron, J. M. 2010. Nanobiocomposites of carrageenan, zein, and mica of interest in food packaging and coating applications. *Journal of Agricultural and Food Chemistry*58(11), 6884–94.
- Tunjano, V., Salcedo, F., Jiménez, I. C., A., M. J., Alvarez, O. A., Prieto, E. 2009. Estudio de las propiedades térmicas y mecánicas del almidón. *Suplemento de la Revista Latinoamericana de Metalurgia y Materiales*S1(1), 29–36.
- Wilhelm, H.-M., Sierakowski, M.-R., Souza, G. P., Wypych, F. 2003. Starch films reinforced with mineral clay. *Carbohydrate Polymers*52(2), 101–110.